Views on Applying RKW Theory: An Illustration Using the 8 May 2009 Derecho-Producing Convective System

MICHAEL C. CONIGLIO

NOAA/National Severe Storms Laboratory, Norman, Oklahoma

STEPHEN F. CORFIDI

NOAA/Storm Prediction Center, Norman, Oklahoma

JOHN S. KAIN

NOAA/National Severe Storms Laboratory, Norman, Oklahoma

(Manuscript received 4 February 2011, in final form 25 October 2011)

ABSTRACT

This work presents an analysis of the vertical wind shear during the early stages of the remarkable 8 May 2009 central U.S. derecho-producing convective system. Comments on applying Rotunno–Klemp–Weisman (RKW) theory to mesoscale convective systems (MCSs) of this type also are provided. During the formative stages of the MCS, the near-surface-based shear vectors ahead of the leading convective line varied with time, location, and depth, but the line-normal component of the shear in any layer below 3 km ahead of where the strong bow echo developed was relatively small (6–9 m s^{-1}). Concurrently, the midlevel (3–6 km) line-normal shear component had magnitudes mostly >10 m s^{-1} throughout.

In a previous companion paper, it was hypothesized that an unusually strong and expansive low-level jet led to dramatic changes in instability, shear, and forced ascent over mesoscale areas. These mesoscale effects may have overwhelmed the interactions between the cold pool and low-level shear that modulate system structure in less complex environments. If cold pool–shear interactions were critical to producing such a strong system, then the extension of the line-normal shear above 3 km also appeared to be critical. It is suggested that RKW theory be applied with much caution, and that examining the shear above 3 km is important, if one wishes to explain the formation and maintenance of intense long-lived convective systems, particularly complex nocturnal systems like the one that occurred on 8 May 2009.

1. Introduction

This study adds to a recent investigation (Coniglio et al. 2011, hereafter CCK11) of the early stages of an intense derecho (Johns and Hirt 1987) that occurred on 8 May 2009 over the central United States. Bow echoes (Weisman 2001) and mesovortices (Miller and Johns 2000; Wheatley et al. 2006) were observed on multiple scales (see Fig. 1). CCK11 focused on a comparison of the meso- and larger-scale environment of the mesoscale convective system (MCS) to that of other MCSs that have occurred over the central United States in late spring. The precipitable water (PW) content, the strength and width of the low-level jet (LLJ), and the 3–6-km lapse rates of the environment were highly anomalous. The combination of these features and modest downdraft convective available potential energy (DCAPE) resulting from high PW and relatively small 0–3-km lapse rates, led CCK11 to infer that mesoscale factors contributing to *updraft* strength, rather than downdraft strength alone, played a significant role in generating strong winds at the surface and maintaining this MCS (see CCK11 for more details).

The main goal of the present study is to detail the environmental shear during the early evolution of the 8 May 2009 event more so than what is presented in CCK11 and to address the possible relevance of cold pool–shear

Corresponding author address: Dr. Michael C. Coniglio, National Severe Storms Laboratory, Rm. 2234, National Weather Center, 120 David L. Boren Blvd., Norman, OK 73072.
E-mail: michael.coniglio@noaa.gov

DOI: 10.1175/MWR-D-11-00026.1

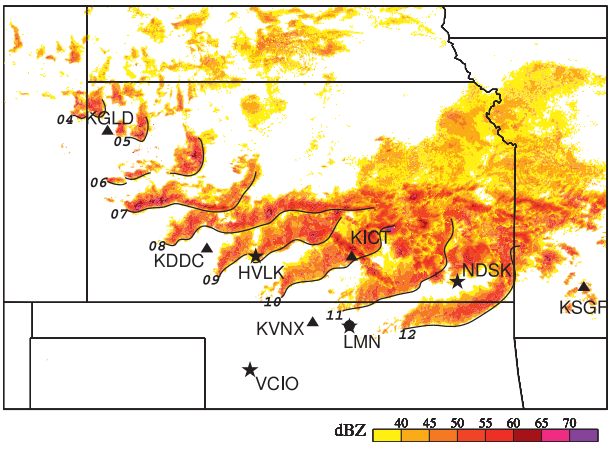

FIG. 1. Hourly composite reflectivity ≥35 dBZ from 0400 to 1200 UTC 8 May 2009 derived from the NMQ project (Vasiloff et al. 2007). Included are the locations and identifiers of the 915-MHz wind profiler sites (filled stars, ★), WSR-88D sites (filled triangles, ▲), and radiosonde sites (filled circles, ●) used in this study and the approximate location of the leading edge of the main convective cluster–line at each hour.

effects, mostly those described by "RKW theory."[1] RKW theory provides a solid foundation to explain idealized squall lines and the basic structure of cold-pool-forced convection, and is often cited in an attempt to explain the strength and structure of a variety of MCS types. A clean application of RKW theory to this event is challenging, because of the usual difficulty in assessing cold pool properties from routine observations (Bryan et al. 2005), but also because of the complexity of the convective evolution and the mesoscale environment. As shown in CCK11 and herein, the 8 May 2009 MCS does not adhere closely to Houze et al.'s (1989) two-dimensional archetype. It also has some characteristics of "type II" MCSs described in Fritsch and Forbes (2001), in which an evolving LLJ impinges on the equatorward side of the system within a developing (albeit rather weak) low-level baroclinic zone. The influence of the mechanisms described by RKW theory may be reduced in these situations (Fritsch and Forbes 2001). Although application of RKW theory is challenging for these reasons, we illustrate that, if cold pool/shear interactions were critical to the MCS evolution, the shear above 3 km may have been important because of relatively weak line-normal shear below 3 km.

Another goal of this work, addressed in section 2, is to review recent updates to RKW theory from the perspective of one who attempts to apply it in a forecast setting. An analysis of the environmental vertical wind shear during the development and upscale growth of the 8 May 2009 derecho-producing MCS follows in section 3. Section 4 provides a summary and some concluding remarks.

2. Application of RKW theory

The primary intent of RKW was to explain how ordinary thunderstorms, with lifetimes of 30–50 min, could be regenerated most effectively by cold pools in homogeneous environments, and why this process seemed to be enhanced by low-level vertical wind shear. RKW argued that the overwhelming influence of cold pools in shearless flow could be countered by low-level vertical wind shear, and the deepest lifting occurs if the circulation associated with the positive vorticity of the low-level shear approximately balances the circulation associated with the generation of negative vorticity by the cold pool. To represent this vorticity balance quantitatively, RKW used the horizontal vorticity equation with simplifying assumptions to arrive at $C = \Delta u$, where C is a measure of the strength of the convectively generated cold pool and Δu is a measure of the ambient vertical wind shear perpendicular to the convective line.

In simulations using the Klemp–Wilhelmson (KW) model (Klemp and Wilhelmson 1978), squall lines were generally most intense and long lasting ("optimal") when $C/\Delta u \approx 1$. Within this framework, $C/\Delta u > 1$ is associated with upshear-tilted and cold-pool-dominated systems and $C/\Delta u < 1$ is associated with shear-dominated systems with more discrete convective structures. In some upshear-tilted systems, elevated LLJs can develop and impinge on the convective line from behind. The import of positive horizontal vorticity associated with the LLJ may alter the associations between $C/\Delta u$ and system structure such that systems may be more upright and intense with the elevated LLJ than they would otherwise be without it (Weisman 1992). Although these associations were derived in two dimensions, Weisman et al. (1988), Weisman and Rotunno (2004, hereafter WR04), and Bryan et al. (2006) show that the concept also applies strongly to idealized squall lines in three dimensions.

a. Shear-depth uncertainties

The criterion $C/\Delta u$, and the KW-model simulations that show how squall lines change as $C/\Delta u$ varies, have provided a way to apply RKW theory. Although the appropriate depth to calculate Δu was not stated explicitly by RKW, they argued that it was the shear within the air that makes contact with the cold pool that was influential (Rotunno et al. 1988, p. 477). This statement

[1] "RKW" refers to the authors of Rotunno et al. (1988). The reader is referred to that paper, Weisman and Rotunno (2004), Stensrud et al. (2005), and Bryan et al. (2006) for a thorough review of RKW theory.

has been interpreted to mean that Δu should be evaluated only over the approximate depth of the cold pool [~2–3 km in the simulations presented in RKW and Weisman et al. (1988)], even if shear extends to levels above the depth of the cold pool. Accordingly, Weisman et al. (1988) calculated Δu over the lowest 2.5 km (the approximate cold pool depth), even if the shear extended to 5 km. This approach was followed in many later studies that attempted to apply RKW theory (e.g., Rotunno et al. 1990; Fankhauser et al. 1992; Grady and Verlinde 1997; Evans and Doswell 2001).

However, using an updated KW model and larger domains, WR04 showed a better correspondence to simulated convective structures when Δu was calculated over the lowest 5 versus 2.5 km, meaning that $C/\Delta u \approx 1$ for the strongest and nearly upright systems when Δu was calculated over the lowest 5 km. For the WR04 simulations, if only the shear over the lowest 2.5 km is used to calculate Δu regardless of the depth of the shear layer (as was originally done in Weisman et al. 1988), measures of squall-line strength were maximized for $C/\Delta u \sim 1.4$–3.4 (see p. 376 of WR04). This is not consistent with the original RKW concept where only the shear that makes contact with the cold pool matters. Therefore, the WR04 three-dimensional simulations imply that it is important to examine the shear over a deeper layer than the cold pool itself to best fit the RKW paradigm.

The recommendation by WR04 to look in deeper layers than recommended by RKW was not because the newer simulations produced deeper cold pools. Rather, it was attributed to two possible factors: 1) the interaction of the elevated shear with the negative buoyancy associated with rain loading in the decaying convective cells above the cold pool and 2) the circulation associated with the positive vorticity of a ''marginally elevated shear layer... acts at a distance to produce enhanced lifting'' (see p. 366 of WR04), meaning the cold pool circulation can impact the flow above the depth of the cold pool. Although the underlying concept may not be the same, the importance of the deeper shear in explaining various characteristics of squall lines was recognized in other studies as well (Fovell and Dailey 1995; Fovell and Tan 1998; Coniglio and Stensrud 2001; Coniglio et al. 2006).

b. Cold pool uncertainties

Along with an appropriate depth over which to calculate Δu, any strict application of RKW theory requires knowledge of the cold pool properties to estimate C. Bryan et al. (2004) and Bryan and Parker (2010) show that cold pools within central U.S. MCSs are sometimes 3–4 km deep. This raises some questions about how the RKW concepts should be applied when the cold pools are deeper than those produced in the simulations that validate RKW theory. The cold pools in the WR04 simulations were generally 1.5–3 km deep, yet WR04 recommend looking at the shear over the lowest 5 km to evaluate the RKW concepts, meaning the ratio of the shear depth that best fits the RKW optimal paradigm to the simulated cold pool depth is ~2:1. When applying these results to real cold pools that are 3–4 km deep, does this mean that the shear should be examined over the lowest 6–8 km to encompass the RKW effects?

If so, this is consistent with observations that show deep shear values (6 km or greater) discriminate strong and long-lived MCSs from weak and shorter-lived MCSs better than do low-level shear values (Cohen et al. 2007; Coniglio et al. 2007). Further, Stensrud et al. (2005) and Weisman and Rotunno (2005, hereafter WR05) show that for strong, deep cold pools, the shear magnitudes that are usually observed in central U.S. MCSs occur in a range in which the lifting by deep-layer shear and low-level-only shear are nearly the same within the two-dimensional vorticity streamfunction analysis of WR04. So, the debate about low-level-only shear versus deep-layer shear emphasized in Weisman et al. (1988) and in WR04 may be largely irrelevant for the strong, deep cold pools that may typify central U.S. MCSs (Bryan et al. 2005; Engerer et al. 2008).

c. Comparison of RKW theory to observations

Following similar analyses in RKW and Weisman (1993), WR05 claim much correspondence between RKW theory and observations of many types of real squall lines (see Table 1 in WR05 and the associated discussion). However, only one of these cases, the 22 May 1976 squall line studied by Ogura and Liou (1980) and Smull and Houze (1987), is the type that is relevant to the current study, namely a strong midlatitude leading-line–trailing-stratiform MCS that existed without well-defined external synoptic-scale forcing (CCK11).

Bryan et al. (2004) analyzed nine Bow Echoes and MCV Experiment (BAMEX; Davis et al. 2004) cases in which pairs of radiosonde observations could be used to compare the MCS cold pool strength to the ambient shear. Their analysis ''supports—or, at least, does not contradict—the main element of RKW theory,'' referring to WR04's claim that system structure is strongly influenced by the relative strength of the system's surface-based cold pool and the shear below 5 km. Similar conclusions are reached in Bryan and Parker (2010).

Studies following RKW (Weisman et al. 1988; Weisman 1993; WR04; Bryan et al. 2006) attempted to define in more detail the changes in system strength, structure, and life cycle as Δu was increased over various layers in three-dimensional KW model simulations. We emphasize that these results may be more applicable to real-world

forecasting than are the results of a particular set of $C/\Delta u$ criteria that produces ''optimal'' squall lines in simulations. Nonoptimal squall lines in the $C/\Delta u$ framework can still be strong and long lived and are therefore still relevant to severe weather forecasting (Evans and Doswell 2001; WR05). Modeling studies following RKW show that simulated systems can produce severe winds (>26 m s^{-1}) at the lowest model level for Δu as low as 10 m s^{-1}, especially when the CAPE is very large (Weisman 1993; WR04).

However, it is important to examine the structural characteristics of these simulations if one is to forecast a certain MCS structure based on the results from the idealized simulations. The parent convective structures for relatively weak values of shear (10 m s^{-1}), which may still produce severe winds, consist of ''upshear-tilted multicells scattered behind the leading edge of the cold pool'' for all shear depths (see Table 1a in WR04). The WR04 simulations suggest that if the shear is initially confined entirely to the lowest 2.5 km (roughly the cold pool depth), then Δu of at least 15 m s^{-1} is needed to begin to produce ''a predominantly upright system with linear or bow-shaped segments of cells just behind the leading edge of the cold pool.'' When the shear extends to 5 km in the WR04 simulations, bow echoes do indeed form when the line-normal shear in the lowest 2.5 km is at least 10 m s^{-1} (as arises for a profile with 20 m s^{-1} over 0–5 km). However, the well-organized bow-echo systems (like the one observed for the 8 May 2009 event) are more prevalent for the stronger, shallow, surface-based shears [$\sim$20 m s^{-1} (2.5 km)$^{-1}$] compared to the 5-km shear depths, and no form of bow echoes develop in the WR04 experiments when the shear is extended to 7.5 and 10 km (see their Table 1a).

It is common to observe magnitudes of Δu lower than 15–20 m s^{-1} over the lowest 2.5–5 km in bow-echo and MCS environments and for shear to extend well above 5 km (Evans and Doswell 2001; Gale et al. 2002; Coniglio et al. 2004; Cohen et al. 2007; Coniglio et al. 2007; Coniglio et al. 2010). This has led some to argue that factors other than the cold pool–low-level shear effects may be important in these cases. The implication for forecasters is twofold. It is important to consider a number of factors beyond whether the shear is optimal according to RKW theory (Stensrud et al. 2005, WR05). It is also important to consider many factors beyond how the observed CAPE and low-level shear magnitude fit into the results of idealized squall-line simulations for similar values of CAPE and shear (Evans and Doswell 2001; Coniglio et al. 2004).

It should be noted that the exact amount of Δu needed to produce well-organized bow echoes depends on the thermodynamics of the environment (Weisman 1993). Furthermore, Bryan et al. (2006) found that the optimal shear for simulations that use newer model frameworks tends to be a little less than those reported in WR04 because the KW model produces cold pools that are somewhat too strong and deep for the thermodynamic conditions. As a result, the minimum values needed to produce organized systems and bow echoes in Weisman (1993) and WR04 may be artificially high compared to those needed in other model frameworks.

It should also be noted that, when Δu is relatively small, RKW theory does predict upshear-tilted systems, and it is recognized that such systems are often still strong and long lived. However, the dynamical response that produces an elevated rear-inflow jet and bow-echo structures in the KW model simulations only occurs for relatively large values of Δu, especially when Δu is confined to the lowest 2.5 km. The simulated squall lines in WR04 for which the 0–3-km line-normal shear is <10 m s^{-1} do indeed tilt upshear, but they never develop the strong elevated rear inflow that is needed to develop well-organized, persistent bow echoes, regardless of the depth of the shear layer. Therefore, in a comparison to a real cold-pool-forced MCS, if the 0–3-km line-normal shear is observed to be <10 m s^{-1}, yet the system is strong and long lived with bow echo structures that are only observed for much larger Δu in the simulations that are used to isolate and validate the RKW concepts, then it is reasonable to inquire if processes other than those described in the RKW concepts are operating.

The intent of the next section is to illustrate the above viewpoint using observations of the 8 May 2009 MCS, which presents the type of analysis that inspired the contention (Stensrud et al. 2005) that the RKW concept may not be the primary influence for many central U.S. MCSs. CCK11 presented several mesoscale factors that could have contributed to the strength of the system. Going forward, we hypothesize on the relevance of cold pool–shear effects given the analysis of environmental shear.

3. Evaluation of RKW theory during the 8 May 2009 MCS

Radar reflectivity data from the Weather Surveillance Radar-1988 Doppler (WSR-88D) network and the National Mosaic and Multisensor Quantitative precipitation estimation (NMQ) project (Vasiloff et al. 2007) were used to analyze the convective evolution. Quality-controlled surface and upper-air observations and hourly 20-km Rapid Update Cycle (RUC) analyses (Benjamin et al. 2004) were used to characterize the environment (see CCK11 for more details on the analysis methods).

When applying RKW theory, it is the component of the shear vector that is perpendicular (normal) to the

convective line–cold pool that is relevant. To calculate the line-normal shear (symbolized by Δu hereafter), six points are defined along the extent of the leading edge of the system beginning at 0600 UTC—the time when a convective line of nearly contiguous reflectivity ≥35 dBZ can be roughly defined—through 1200 UTC, when a well-organized bow echo was occurring. The RUC grid points ahead of the leading line are populated with azimuth angles constructed from a horizontal interpolation of radials that are directed outwardly normal from the six defined points along the convective line. The maximum component of line-normal shear in any layer between two height levels ($\Delta u_{\max}$) is then computed along these interpolated radials and is displayed at grid points up to 300 km ahead of the convective line. As detailed below, $\Delta u_{\max}$ is calculated over different depths that could represent possible cold pool depths, as well as for deeper layers, based on the uncertainties in applying the theory discussed in section 2.

a. Initial convection and MCS development

The initial convective development occurred in Colorado between 0000 and 0400 UTC and was likely elevated (see CCK11 and Figs. 1 and 2). The available surface observations (Fig. 3a) and WSR-88D data show that the convective development after 0400 UTC occurred along convective outflow. The strongest convection developed along the portion of the outflow that had the largest angle to the shear vectors through 0600 UTC (Fig. 4). This is consistent with the main point of RKW theory—the convection was strongest where the shear was nearly perpendicular to the cold pool. However, the character of the convection and the relationship of the convection to the shear became much more complex after 0600 UTC as the system intensified.

By 0700 UTC, storm coverage and intensity had increased rapidly over western Kansas along the western portion of the outflow (Fig. 3b). The strong cell along the eastern extent of the cluster of cells at 0600 UTC (Fig. 3a) had weakened. The mode transitioned from clusters of cells at 0600 UTC into a linear MCS with an east–west orientation by 0700 UTC (Fig. 3b). Surface temperatures dropped 5–7 K between 0600 and 0700 UTC (Fig. 3), indicating that a cold pool was present prior to 0700 UTC.[2]

Meanwhile, an LLJ was intensifying to the south and tapped a reservoir of very moist air over western Oklahoma and the Texas Panhandle, transporting it northward through 0900 UTC (Fig. 5). WSR-88D data revealed that the strong east–west-oriented convection at 0700 UTC developed along outflow that surged southward from the cluster of cells at 0600 UTC and encountered an LLJ that was anomalously strong and wide (Fig. 6).

Between 0700 and 0800 UTC, the northward moving air mass that collided with the cold pool (Fig. 3) appeared to introduce a deeper layer of instability rooted closer to the surface on the southern flank of the system, as supported by the CAPE and convective inhibition (CIN) fields (Fig. 2). The surface-based CIN near the convective line continued to be relatively large at 0800 UTC (Fig. 2d), but the mixed-layer CIN (MLCIN) became quite small (>-50 m^2 s^{-2}) by 0800 UTC (Fig. 2e), reflecting the shallower surface stable layer within the northward-moving air mass. The statically stable surface layer within this air mass was only about 500 m deep and was not particularly cool at 0500 UTC (Fig. 7).

b. Depths used in the calculation of $\Delta u_{\max}$

Given the shallowness and weakness to the nocturnal inversion, it is possible that some near-surface parcels were being ingested into convective updrafts. After 1000 UTC, the MLCIN increases once again (Fig. 8), so if a significant mass of near-surface air was being ingested, the duration of this process may have been limited to a period between 0700 and 1000 UTC. Thus, recognizing that the parcels within the weak surface stable layer may not be part of the effective inflow layer, and to be most relevant in a comparison to the WR04 simulations, the low-level shear calculations are based at 0.5 km. The near-surface winds are deemphasized because the use of the 10-m analyzed wind resulted in low-level shear vectors oriented *parallel to and even directed toward the system*, rendering the 0–3-km line-normal shear below zero in many locations [see the wind profiles at Haviland, Kansas (HVLK) and Lamont, Kansas (LMN), in Figs. 9 and 10 herein, and Fig. 17 of CCK11 for 0–3-km shear vectors at 0700 UTC].

We examined the maximum line-normal shear ($\Delta u_{\max}$ hereafter) based at 0.5 km for a range of upper bounds from 2 to 6 km. This range is designed to span a range from the typical cold pool depths in the WR04 idealized simulations (2–3 km) to depths that are likely well above the top of the cold pool (6 km). For brevity, $\Delta u_{\max}$ is only displayed for the 0.5–3- and 0.5–6-km layers. These two layers are illustrated for a few reasons. Although WR04 examined shear over the lowest 2.5 and 5 km, we chose 3 and 6 km recognizing that cold pools in

[2] Note, however, the portion of the convective line between 0700 and 0800 UTC depicted by the red-dashed line in Fig. 3c developed along a northward-moving moisture discontinuity identified as a fine line in WSR-88D imagery (CCK11). The development of convection along this boundary should not be immediately included in the analysis of RKW concepts since it was apparently not forced by the preexisting cold pool, at least not prior to 0800 UTC.

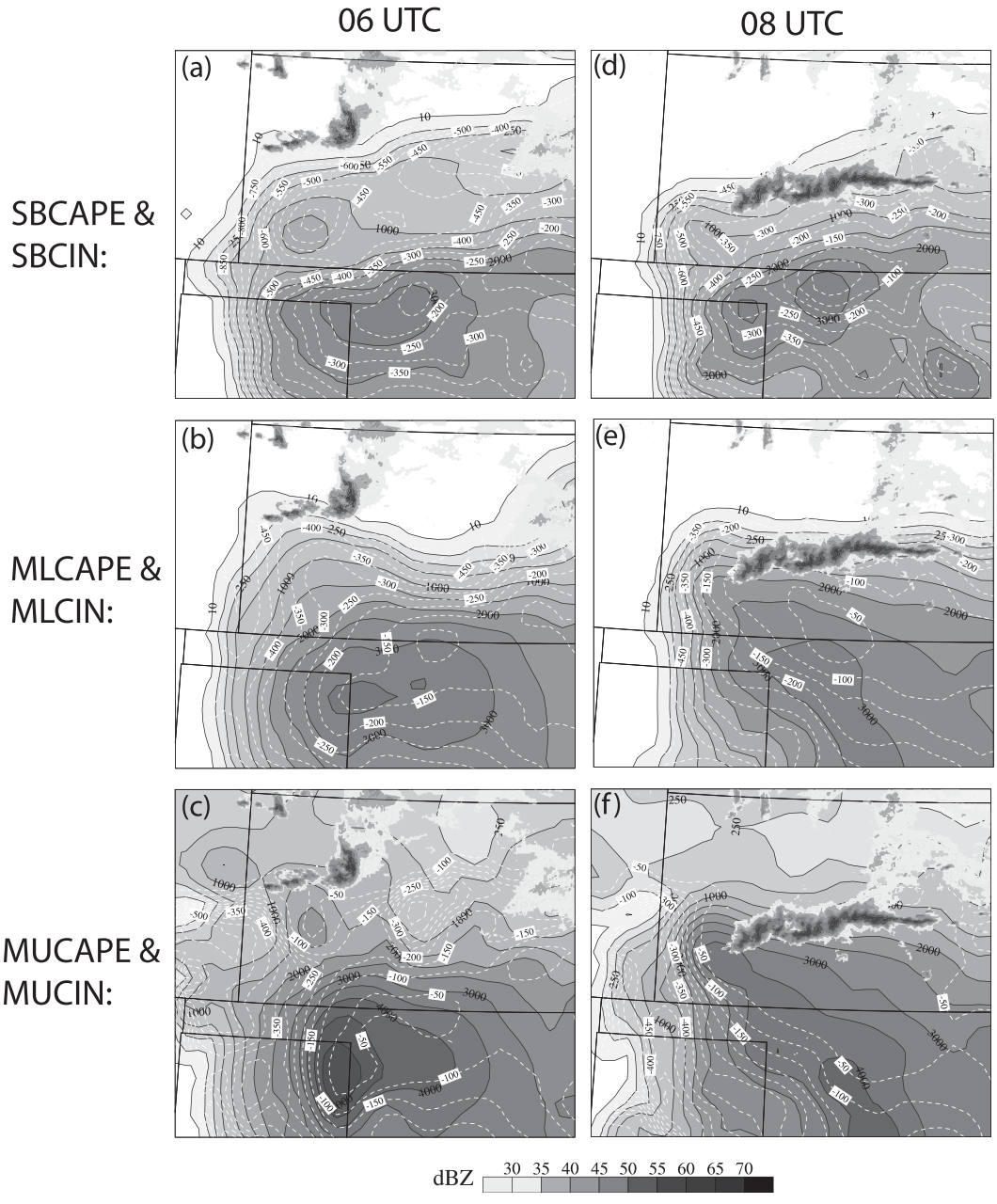

FIG. 2. RUC analyses of CAPE and CIN ($m^2\ s^{-2}$) for (top) a surface parcel (SBCAPE and SBCIN), (middle) a parcel mixed over the lowest 100 hPa (MLCAPE and MLCIN), and (bottom) the most-unstable parcel in the lowest 300 hPa (MUCAPE and MUCIN) valid at (left) 0600 and (right) 0800 UTC. Contours of CAPE are drawn and shaded at 10, 100, 250, 500, and every 500 $m^2\ s^{-2}$ thereafter. Contours of CIN (white dashed lines) are drawn at -25, -50, -100, -150, -200, and every -100 $m^2\ s^{-2}$ thereafter up to -500 $m^2\ s^{-2}$. Composite reflectivity ≥25 dB*Z* from the NMQ composite reflectivity mosaic also is shown.

the central United States are likely somewhat deeper than those produced in the WR04 simulations. Furthermore, the shears over the lowest 3 and 6 km are most often used in operational forecast settings for a variety of applications, and, historically, the shear over the lowest 3 km is used frequently in applications of the RKW concepts to MCS forecasting. For example, the matrix of convective-system types for a CAPE and 0–2.5-km Δu parameter space shown in Weisman (1993) has been emphasized in National Weather Service forecaster training for many years (UCAR 2010a,b) and shear over the lowest 2–3 km is cited in a discussion of applying

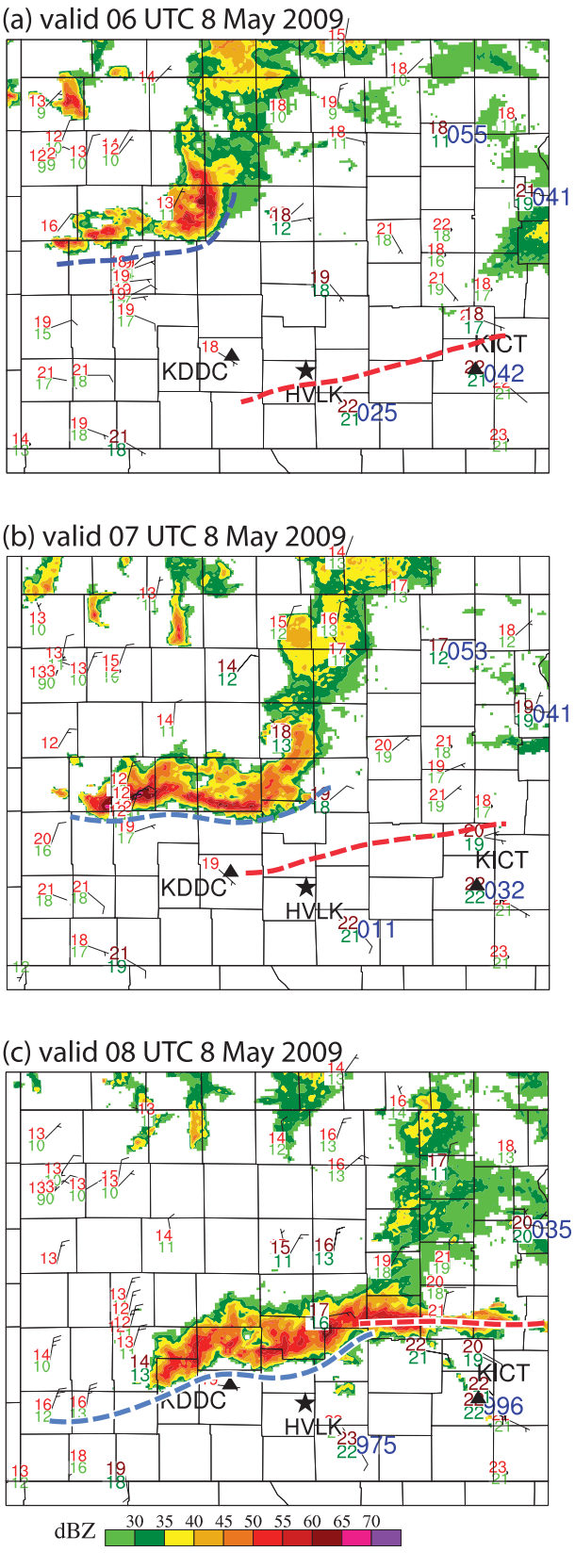

RKW theory in Markowski and Richardson (2010, p. 257), although they did acknowledge some drawbacks to using the 0–2.5-km layer.

We also examined Δu_{max} over layers based at 3 and 4 km to examine the shear in layers elevated above the cold pool, and display the 3–6-km Δu_{max}. The 3–6-km shear is displayed to allow a comparison to a recent investigation (Coniglio et al. 2010) that shows the shear in this layer is a good discriminator of short- and long-lived MCSs (larger 3–6-km shear is found for longer-lived systems) and because the lapse rates in this same layer were found to be highly anomalous for this event (CCK11).

c. Δu_{max} at 0700 and 0800 UTC

At 0700 UTC, values of Δu_{max} over the deepest near-surface-based layers considered were substantial, ranging from 18 to 25 m s^{-1} along and ahead of the line (Fig. 11a). This is consistent with the values of 0–5-km shear that produce strong squall lines in the WR04 simulations. However, the shear in the lower half of this layer is quite variable and tells a different story. The 0.5–3-km Δu_{max} generally increases along a radial outward from just ahead of the convective line but also varies significantly from west to east along the line (Fig. 11b). At 0700 UTC, values of 0.5–3-km Δu_{max} were largest along the western portion of the line and were generally 15–20 m s^{-1}. The values dropped to near 7 m s^{-1} along the center (and strongest) portion of the line before increasing again to around 15 m s^{-1} along the northeastern edge of the line (which may not have been forced by the cold pool at this time) (Fig. 11b). The spatial distribution of 3–6-km Δu_{max} countered that seen for the 0.5–3-km shear, with the smallest values found along the western portion of the line (3–6 m s^{-1}) and the largest values found along the eastern portion of the line (9–12 m s^{-1}).

The shear varied along the line over all layers at 0800 UTC (Fig. 12). The values of 0.5–6-km Δu_{max} were largest ahead of the western portion of the line (22–25 m s^{-1}) and dropped to around 15 m s^{-1} ahead

←

FIG. 3. (a)–(c) Surface observations and NMQ composite reflectivity ≥25 dBZ valid 0600–0800 UTC 8 May 2009. The surface observations include 2-m temperature (°C) in red, 2-m dewpoint (°C) in green, sea level pressure (hPa) in blue, and winds (full barb every 5 m s^{-1}). The blue dashed line indicates the leading edge of the convectively generated cold pool and was determined by examining the surface observations and WSR-88D data from Dodge City, KS (KDDC). The dashed red line indicates a fine line observed in KDDC and KICT WSR-88D data. The darker colors and bigger font depict aviation routine weather report (METAR) observations and the lighter colors and smaller font depict observations from various mesoscale observation networks.

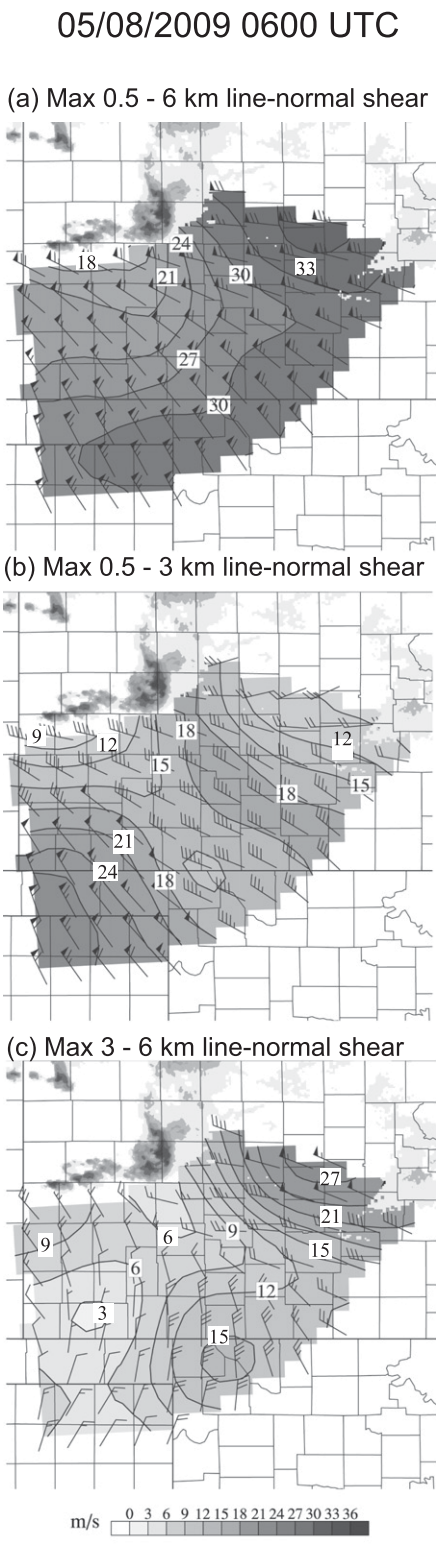

FIG. 4. Maximum magnitude of the vertical wind shear normal to the convective line over the (a) 0.5–6-, (b) 0–3-, and (c) 3–6-km layers shaded and contoured every 3 m s^{-1} from the RUC analysis valid 0600 UTC 8 May 2009. Barbs represent the shear vector within the Δu_{max} layer (full barbs = 5 m s^{-1}, pennants = 25 m s^{-1}).

of the eastern portion of the line (Fig. 12a). Like the spatial distribution of 0.5–3-km Δu_{max} at 0700 UTC, the values of 0.5–3-km Δu_{max} at 0800 UTC are largest ahead of the western portion of the line (15–18 m s^{-1}), and smallest ahead of the eastern portion of the line, where the values were as low as 5 m s^{-1}. The 0.5–3-km Δu_{max} is relatively small at 0800 UTC because of the veering of the 0.5–1-km winds seen at HVLK (Fig. 9) and at LMN (Fig. 10). The spatial distribution of 3–6-km Δu_{max} again countered that seen for the 0.5–3-km shear, with the smallest values found ahead of the western portion of the line (6–9 m s^{-1}) and the largest values found ahead of the eastern portion of the line (12–15 m s^{-1}) (Fig. 12c).

d. Bow-echo development

By 0900 UTC, the system grew in size and developed trailing stratiform precipitation behind the northeastern portion of the system. Meanwhile, the main convective line (labeled A in Fig. 13) developed a line-echo-wave pattern (LEWP; Nolan 1959) and became oriented west-southwest to east-northeast. Additional bands of convection (labeled B, C, and D in Fig. 13) had developed ahead of the main convective line in a northwest-to-southeast orientation.

A zoomed-in view of the area near the intersection of lines A and B (Fig. 14) shows that the LEWP appearance resulted from strong downdrafts and locally enhanced outflow winds embedded within the larger convective line (creating small variations in the speed of the gust front). One of these localized embedded areas of enhanced outflow winds that preceded the development of the main bow echo is seen northwest of Wichita, Kansas (KICT) (Fig. 14b). At least two ~10-km wide leading-line mesovortices also developed with this feature; the latter stage of one of them is indicated in Fig. 14b. Meanwhile, larger-scale rear inflow was developing separately farther west (Fig. 14b). This larger-scale rear inflow caught up to the smaller-scale outflow winds and mesovortex near KICT, producing a single, expanding bow echo by 1000 UTC (Fig. 14c). The bow echo continued to expand as it accelerated east-southeastward through far southeastern Kansas and into southwestern Missouri after 1200 UTC (Fig. 13d).

←

Since only the line-normal component is contoured, the speeds indicated on the barbs only match the contoured speeds if the barb is perpendicular to the convective line. Composite reflectivity ≥25 dBZ from the NMQ composite reflectivity mosaic also is shown.

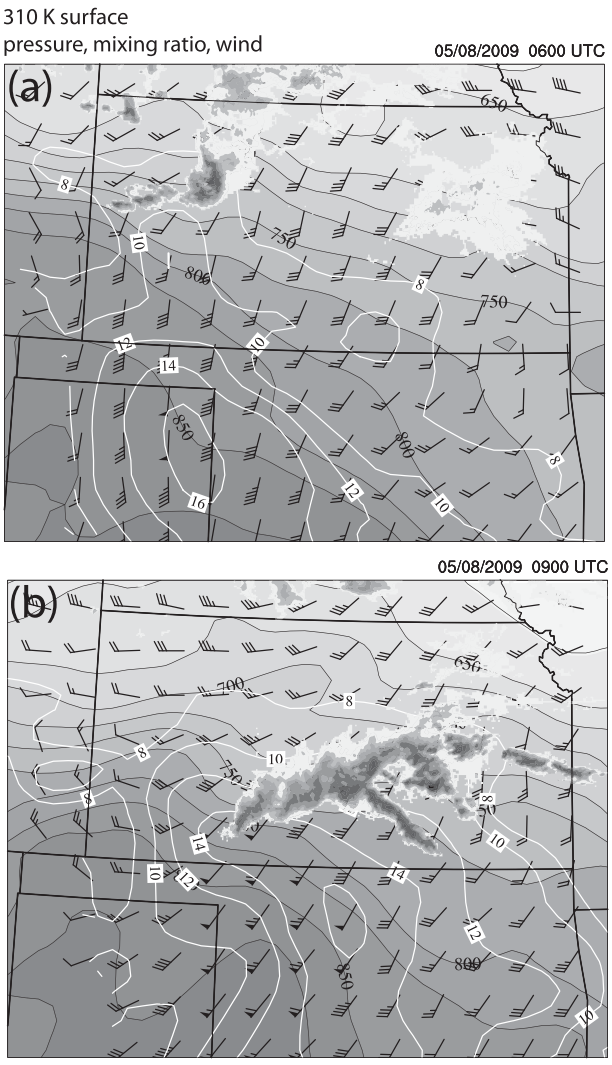

FIG. 5. RUC analysis of pressure shaded and contoured every 25 hPa, mixing ratio contoured every 2 g kg^{-1} starting at 8 g kg^{-1}, and wind vectors (full barb = 5 m s^{-1}, pennant = 25 m s^{-1}) on the 310-K potential temperature surface valid at (a) 0600 and (b) 0900 UTC 8 May 2009. Composite reflectivity ≥25 dBZ from the NMQ composite reflectivity mosaic also is shown.

e. $\Delta u_{\max}$, *0900–1200 UTC*

The shear continued to be variable ahead of the line at 0900 and 1000 UTC (Figs. 15 and 16), with the most variability seen for the values of 0.5–3-km $\Delta u_{\max}$. The distribution of 0.5–3-km $\Delta u_{\max}$ at 0900 UTC continued to show the largest values (~18–20 m s^{-1}) ahead of the western edge of the line to values generally 6–9 m s^{-1} ahead of the eastern portion of the line where the bow echo shown in Fig. 14 subsequently developed (Fig. 15b). Doppler wind profile observations corroborate these values of low-level shear ahead of the line; the 0.5–3-km $\Delta u_{\max}$ at Neodesha, Kansas (NDSK), was only about 6 m s^{-1} at 1000 UTC, which was approximately an hour before the passage of the bow echo (Fig. 17). The NDSK line-relative wind profile (Fig. 17), along with the profiles from earlier in the system's evolution (Figs. 9 and 10), highlight the tendency for much of the shear in the lowest 3 km to be line parallel.

The values of 0.5–6-km $\Delta u_{\max}$ ahead of the line varied from 25 m s^{-1} to the west to about 16 m s^{-1} to the east (Fig. 15a). Accordingly, the spatial distribution of 3–6-km $\Delta u_{\max}$ at 0900 and 1000 UTC again countered that seen for the 0.5–3-km $\Delta u_{\max}$, with the smallest values found along the western portion of the line (6–8 m s^{-1}) and the largest values found along the eastern portion of the line (9–12 m s^{-1}).

The west–east variability in the shear lessens somewhat at 1100 and 1200 UTC (Figs. 18 and 19), with values of 0.5–6-km $\Delta u_{\max}$ being generally between 18 and 22 m s^{-1}, and values of 0.5–3-km $\Delta u_{\max}$ being generally between 7 and 10 m s^{-1} ahead of where the bow echo moves into far southeastern Kansas and southwestern Missouri. The spatial distribution of 3–6-km $\Delta u_{\max}$ also becomes a little less variable with values consistently between 8 and 12 m s^{-1} ahead of the surging bow echo through 1200 UTC.

f. Comparison to idealized simulations

A significant amount of low-level Δu is needed to develop bow echoes within idealized modeling constraints likely because of the importance of significant cold-pool forcing relative to other factors, by design. The cold pool for this event may not have been especially strong compared to other MCSs of this type, judging by the modest evaporative potential in the environment (see Fig. 19 of CCK11). However, surface temperature deficits of 5–7 K were present prior to 0800 UTC (Fig. 3) and were 4–6 K during the bow-echo stage from 0900 to 1200 UTC (Fig. 13), which is typical for nocturnal bow echoes (Adams-Selin and Johnson 2010). This suggests that significant cold pool forcing was present for the event and warrants an attempt to evaluate RKW theory.

For the stage of MCS development prior to the bow echo (before 0900 UTC), the strongest portion of the cold-pool-forced convective line developed rapidly, and stayed strong through 0800 UTC, with intense cells just behind the leading edge of the cold pool despite weak line-normal shear in the lowest 3 km. If one assumes that the cold pool was at least moderately strong and deep (the surface temperature deficits of 5–7 K prior to 0800 UTC suggest that it was), then there is a good possibility that factors other than the near direct interaction of the cold pool with the shear in the environment over approximately the same layer [the mechanism emphasized originally in RKW and Weisman et al. (1988)]

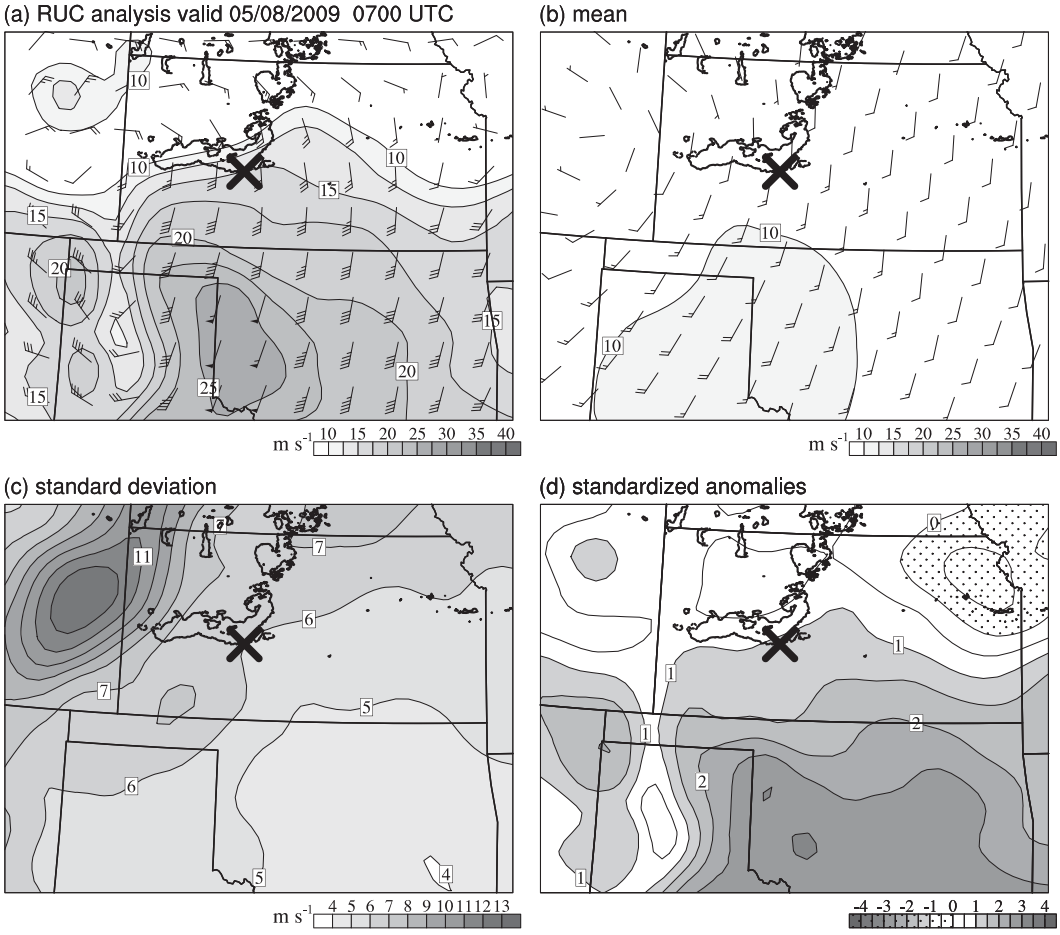

FIG. 6. (a) RUC analysis of 500-m AGL wind speed shaded and contoured every 2.5 m s^{-1}, starting at 10 m s^{-1} (full barb = 5 m s^{-1}, pennant = 25 m s^{-1}) valid 0700 UTC 8 May 2009. The boldface crisscross (×) marks a location near the center of the leading convective line that was used for the comparison of the analysis in CCK11 to the Coniglio et al. (2010) dataset. (b) As in (a), but for the mean 500-m AGL wind speed ahead of the newly developed MCSs from the set of 28 MCSs described in Coniglio et al. (2010), where the boldface crisscross marks the location near the center of the leading convective line that was used in the compositing procedure. (c) As in (b), but for the standard deviation of 500-m AGL wind speed from the set of 28 MCSs shaded and contoured every 1 m s^{-1}, and (d) 500-m AGL wind speed standardized anomalies based on a comparison to the Coniglio et al. (2010) dataset, with the negative anomalies hatched.

contributed to this regeneration of convection along the gust front.

The 0.5–6-km Δu_{max} was more substantial than the 0.5–3-km Δu_{max} prior to 0900 UTC. If cold pool–shear interactions were critical, then this suggests that the extension of the shear to levels well above 3 km was important. Of course, the precise depth of the cold pool is not known, so it is not clear if this extension of the shear above 3 km was important because the cold pool extended well above 3 km, or if processes related to shear that was elevated above the cold pool were important. If it was the latter, convective-scale hypotheses related to this shear elevated above the cold pool are discussed later in section 3g.

If mesoscale factors were critical at this stage, then a possible factor is the strong mesoscale lifting implied by the isentropic ascent over southwest Kansas (Fig. 5) that may have been enhanced along the southward-surging gust front (see CCK11 for more discussion). The moistening and destabilization caused by the LLJ is seen in the comparison of observed soundings taken at LMN (Fig. 7), and is a mechanism long known to play a role in many large, nocturnal MCSs (Maddox 1983; Augustine and Caracena 1994; Trier et al. 2006).

For the bow-echo development stage between 0900 and 1000 UTC, the values of 0.5–3-km Δu_{max} are generally 6–9 m s^{-1} ahead of the portion of the line that develops into the strong well-defined bow echo. The values

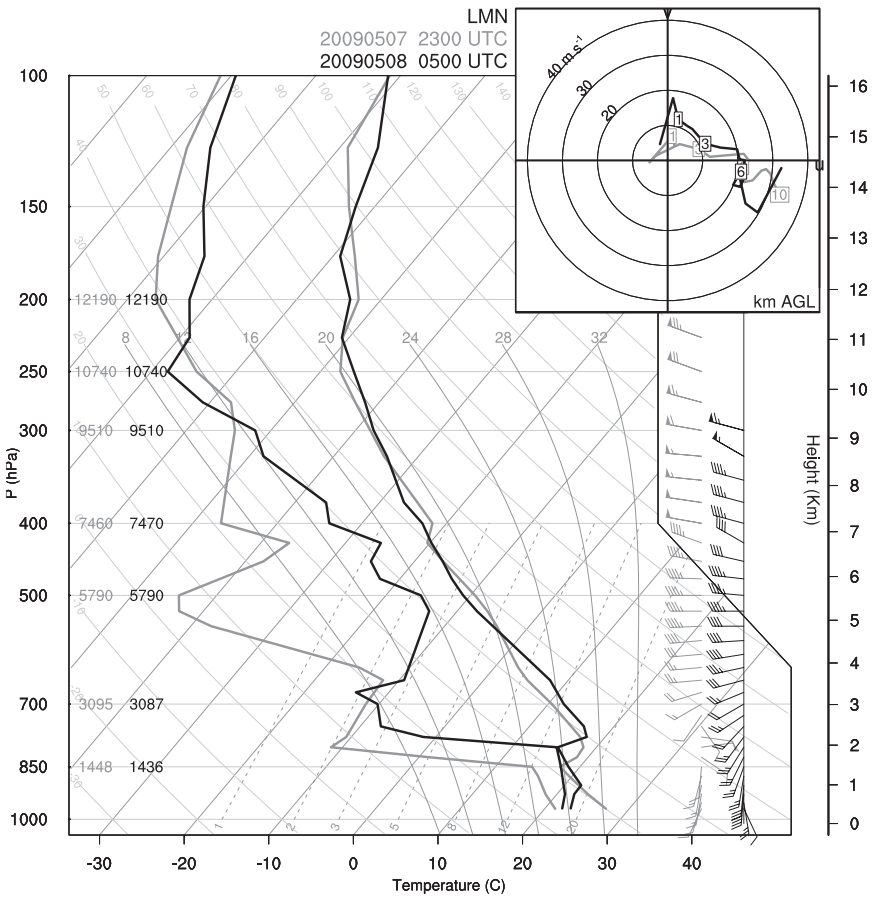

FIG. 7. Skew T–log$p$ diagrams and hodographs from observed soundings at LMN (see Fig. 1 for location) valid at 2300 UTC 7 May 2009 (gray lines) and at 0500 UTC 8 May 2009 (black lines). Full wind barbs represent 5 m s^{-1} and pennants represent 25 m s^{-1}.

of 0.5–3-km $\Delta u_{\max}$ ahead of the expanding bow echo in far southeastern Kansas and far southwestern Missouri became slightly larger from 1100 to 1200 UTC, but remained generally at and below 10 m s^{-1}. As described in section 2, bow echoes develop in the WR04 simulations after the cold pool overwhelms the ambient low-level shear (i.e., $C/\Delta u > 1$). *But well-organized bow echoes only develop if* Δu *calculated over the depth of the cold pool is above a certain value initially:* $\sim$*15–20 m s*$^{-1}$ *if the shear layer is confined entirely to the approximate depth of the cold pool, or* $\sim$*10 m s*$^{-1}$ *if the shear extends to 5 km in the WR04 simulations*. The values of line-normal shear below 3 km along the portion of the line that developed into the bowing system were less than these values. When the shear extends to 5 km in the WR04 simulations, bow echoes do form when the line-normal shear in the lowest 2.5 km is $\sim$10 m s^{-1}, indicating that the extension of the shear layer above the cold pool can be what makes the difference between a weak upshear-tiled system and a strong well-defined bow echo. Indeed, the 3–6-km $\Delta u_{\max}$ values consistently *increase* from west to east ahead of the line, so that less of the 0.5–6-km shear resides below 3 km farther east along the line where the strong well-defined bow echo develops.

g. Alternative hypotheses

We have shown that the 8 May 2009 event, which was a leading line–trailing stratiform bow-echo MCS, developed and matured in an environment with 1) highly variable shear below 3 km ahead of the line, 2) relatively small values of line-normal shear below 3 km, and 3) the largest values of 3–6-km shear along the portion of the line that develops into a strong bow echo. If cold pool–shear interactions were critical, then this suggests that the extension of the shear to levels well above 3 km was important. Again, the precise depth of the cold pool is not known for this event, so it is not clear if the extension of the shear above 3 km was important because the cold pool extended well above 3 km, or if processes related

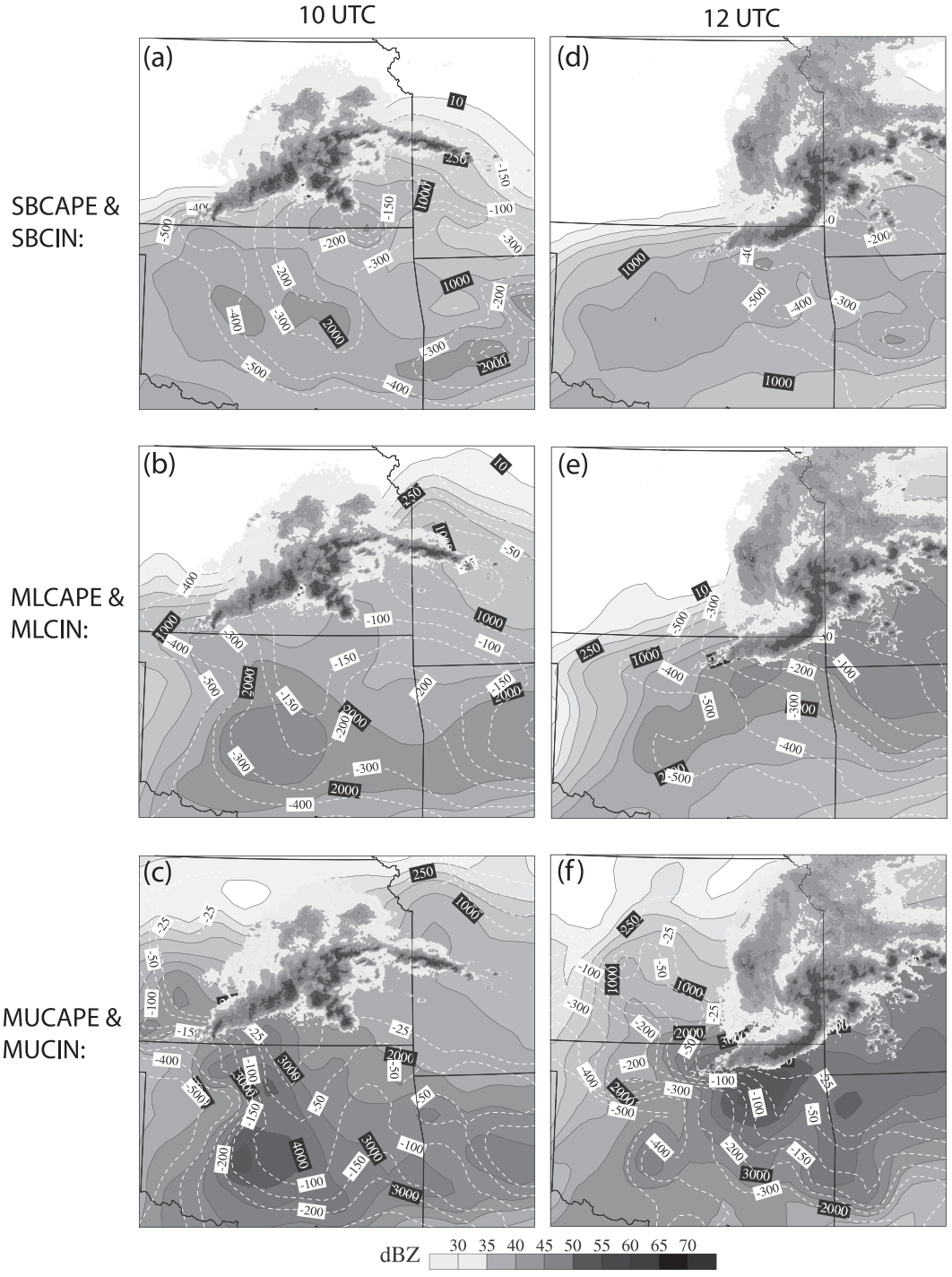

FIG. 8. As in Fig. 2, but valid at 1000 and 1200 UTC.

to shear that was elevated above the cold pool were important.

If the elevated shear was important, many other studies show that this elevated shear can be beneficial to squall lines (Shapiro 1992; Fovell and Dailey 1995; Fovell and Tan 1998; Parker and Johnson 2004; WR04; Coniglio et al. 2006). For example, buoyant updrafts, and their pressure perturbations that can augment the forced updraft along the cold pool (Fovell and Tan 1998), may remain in a favorable location along the cold pool for

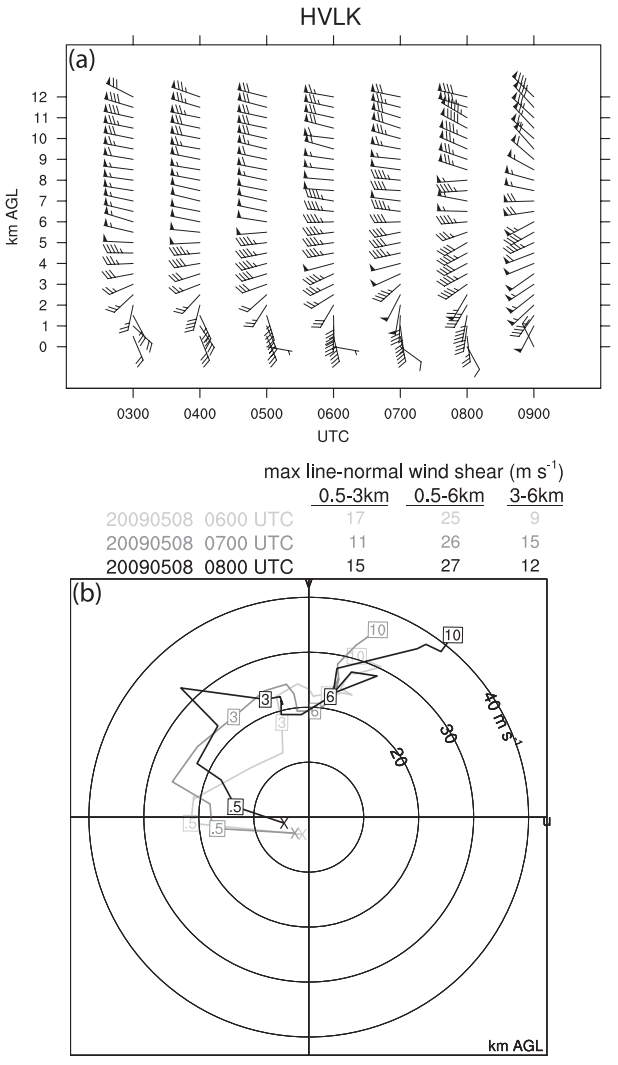

FIG. 9. (a) Hourly wind profile from HVLK from 0300 to 0900 UTC 8 May 2009 (full barb = 5 m s^{-1}, pennant = 25 m s^{-1}) and (b) hodographs of the wind components in a coordinate system with the main convective line oriented along the *y* axis valid at 0600 UTC (light gray line), 0700 UTC (medium gray line), and 0800 UTC (black line). The 10-m wind from the nearest surface station was used for the surface wind. The maximum line-normal wind shear over the 0.5–3-, 0.5–6-, and 3–6-km layers is provided in (b). The MCS reached the HVLK site at approximately 0900 UTC.

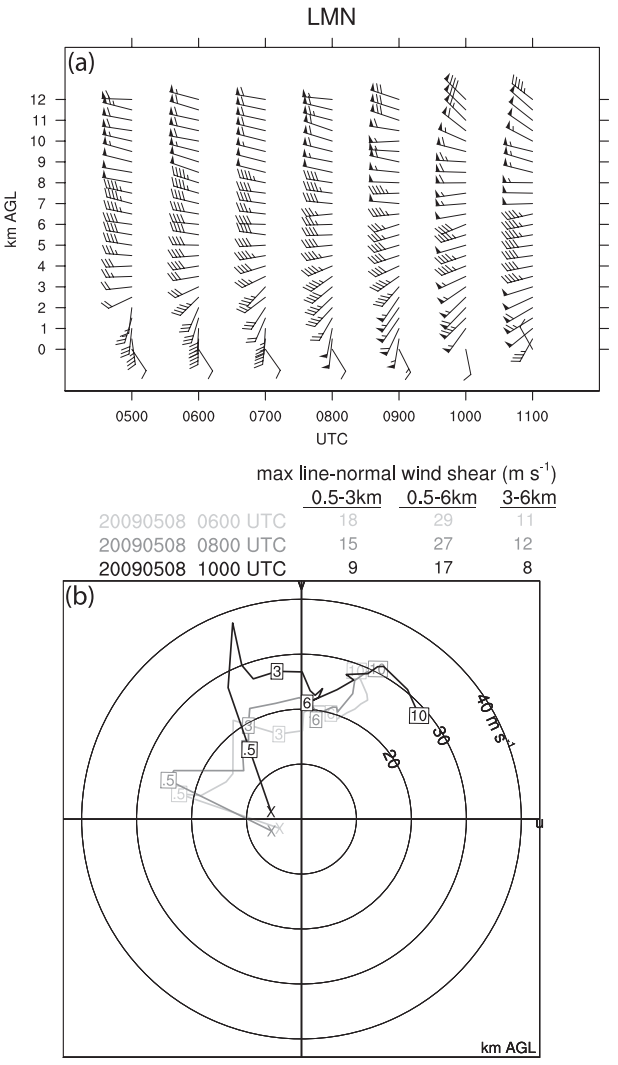

FIG. 10. As in Fig. 9, but at LMN and valid (a) between 0500 and 1100 UTC and (b) at 0600, 0800, and 1000 UTC. The MCS gust front reached the LMN site at approximately 1100 UTC.

long periods within positive elevated shear (Coniglio et al. 2006).

The downshear-directed pressure gradients within updrafts that arise from updrafts in linear shear (Rotunno and Klemp 1982; Parker and Johnson 2004), and the associated enhancement in the lifting of low-level air (Coniglio et al. 2006), may simply cause the subsequent updrafts to be more erect, and ultimately stronger (Parker 2010), than they would otherwise be without the elevated positive shear. In the 8 May 2009 case, the elevated (3–6 km) shear that was consistently oriented perpendicular to the convective line had magnitudes near that which maximizes lifting in idealized simulations of squall lines (8–12 m s^{-1}) (Coniglio et al. 2006). The observational analysis of Coniglio et al. (2010) supports the general importance of the elevated shear. They show that the 3–6-km shear discriminates long-lived from shorter-lived MCSs far better than the surface-based or near-surface-based low-level shear.

Other processes may be related to the highly anomalous 3–6-km lapse rates (see Fig. 18 of CCK11). The large lapse rates could have simply enhanced the updraft strength through positive buoyancy alone, and lessened the impact of the detrimental cold pool circulation (if it was acting above 3 km), regardless of the elevated shear.

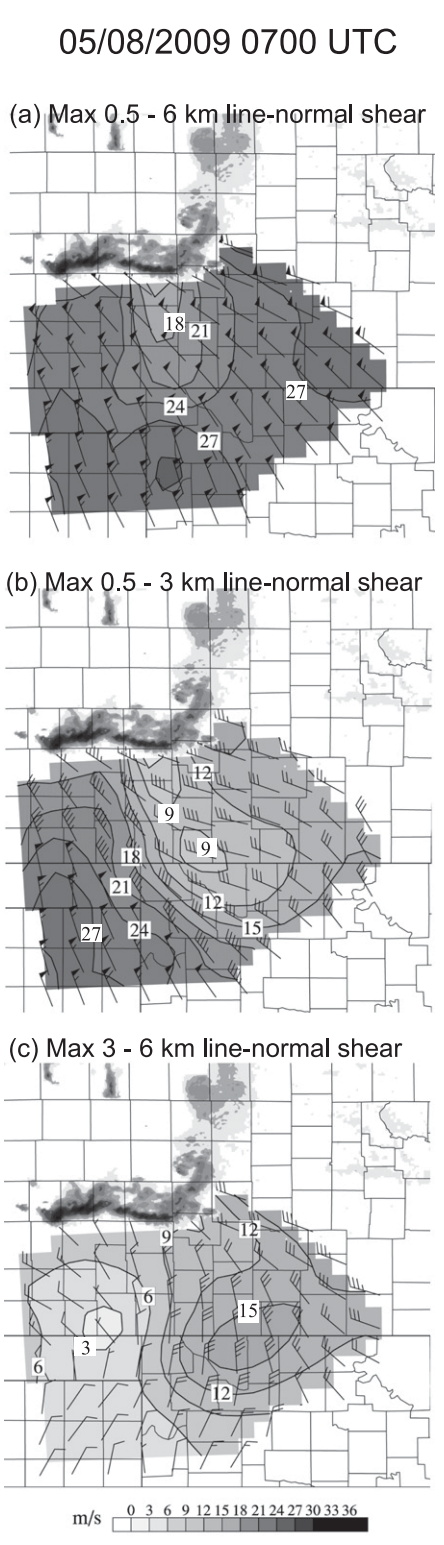

FIG. 11. As in Fig. 4, but valid at 0700 UTC 8 May 2009.

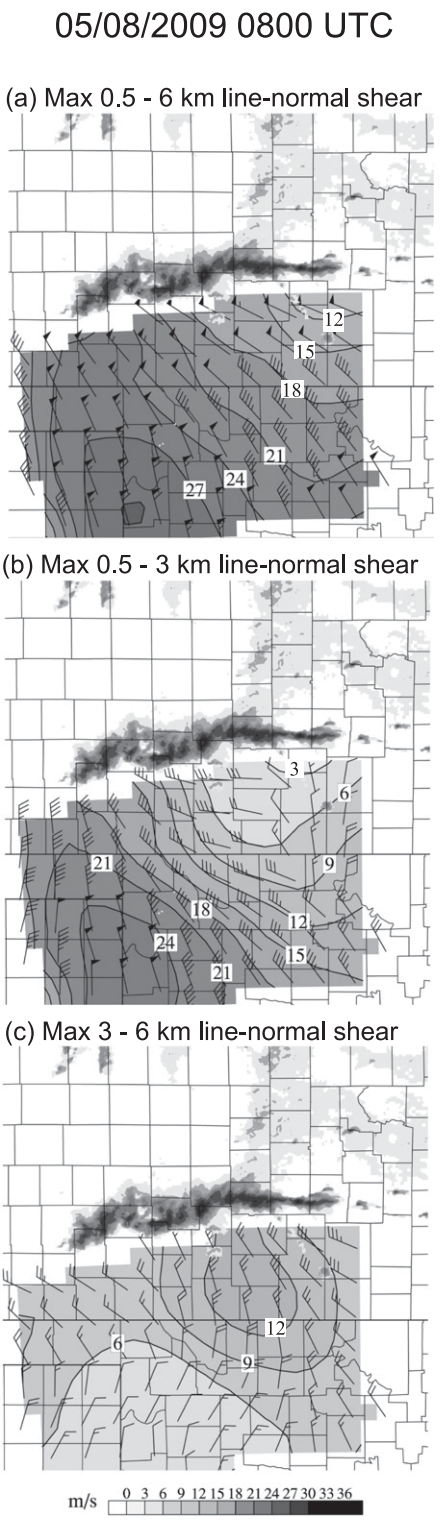

FIG. 12. As in Fig. 4, but valid at 0800 UTC 8 May 2009.

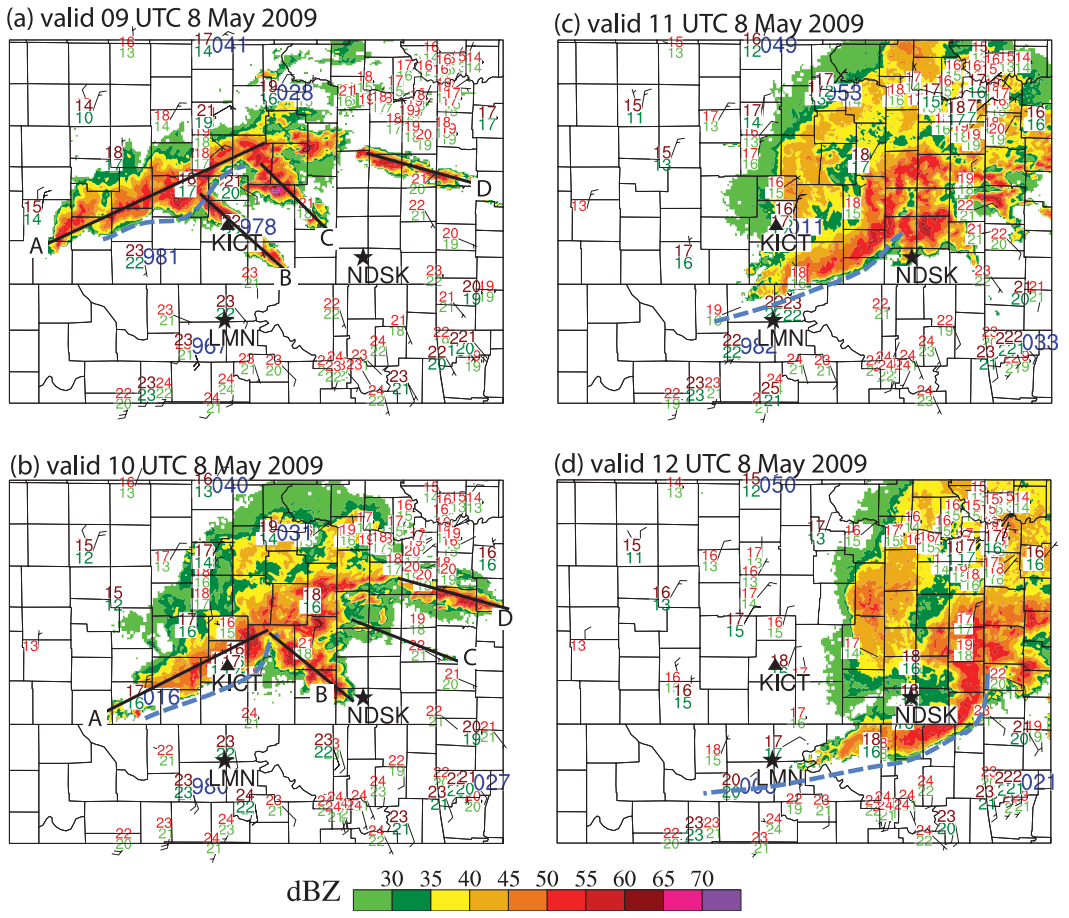

FIG. 13. As in Fig. 3, but valid hourly between 0900 and 1200 UTC. See text for description of the labels A–D in (a) and (b).

It is also possible that the large lapse rates over this same layer made it easier for the ''updraft in shear'' effect to operate as follows. The in-updraft downshear-directed accelerations induced by the updraft-in-shear effect are proportional to the vertical velocity of the updraft (Rotunno and Klemp 1982), which in turn is proportional to the integrated positive buoyancy. Therefore, the enhancement in the positively buoyant updrafts due to the large 3–6-km lapse rates could augment the updraft-in-shear effect by increasing the vertical velocity attained in the buoyant updraft.

The relative importance of the above-mentioned processes related to the elevated shear is not known, or if the explanation lies in a cold pool that was much deeper than 3 km. If the elevated shear processes were important, their cumulative effect could be such that it generates a stronger, nearly upright system in a situation where RKW theory would predict a weaker upshear-tilted system.

Another possible mechanism lies in the mean wind over deep layers, which were strong (Fig. 17) and were generally from the west through 1200 UTC. Although it is difficult to separate the dynamical effects of the mean winds versus the shear in the same layer, recent studies suggest that strong flow in a deep layer above the cold pool could influence the motion of the convective system through vertical momentum transport within the leading portions of the cold pool in a direction along the mean deep-layer wind (Evans and Doswell 2001; Corfidi 2003; Mahoney et al. 2009). The enhanced speed of the cold pool in turn could be enhancing the rate at which the unstable parcels are lifted to their level of free convection along the convergent region between the surging cold pool and the inflow associated with the strong and deep LLJ (Corfidi 2003; French and Parker 2010). Indeed in this case, the flow in the 0–2-km layer was directed at a large angle toward the system and was unusually strong and geographically extensive (Fig. 6), providing very strong inflow into the system. The inflow tapped air with highly anomalous moisture content (see Fig. 17 of CCK11), creating inflow that continuously supplied high-equivalent potential temperature air in low levels.

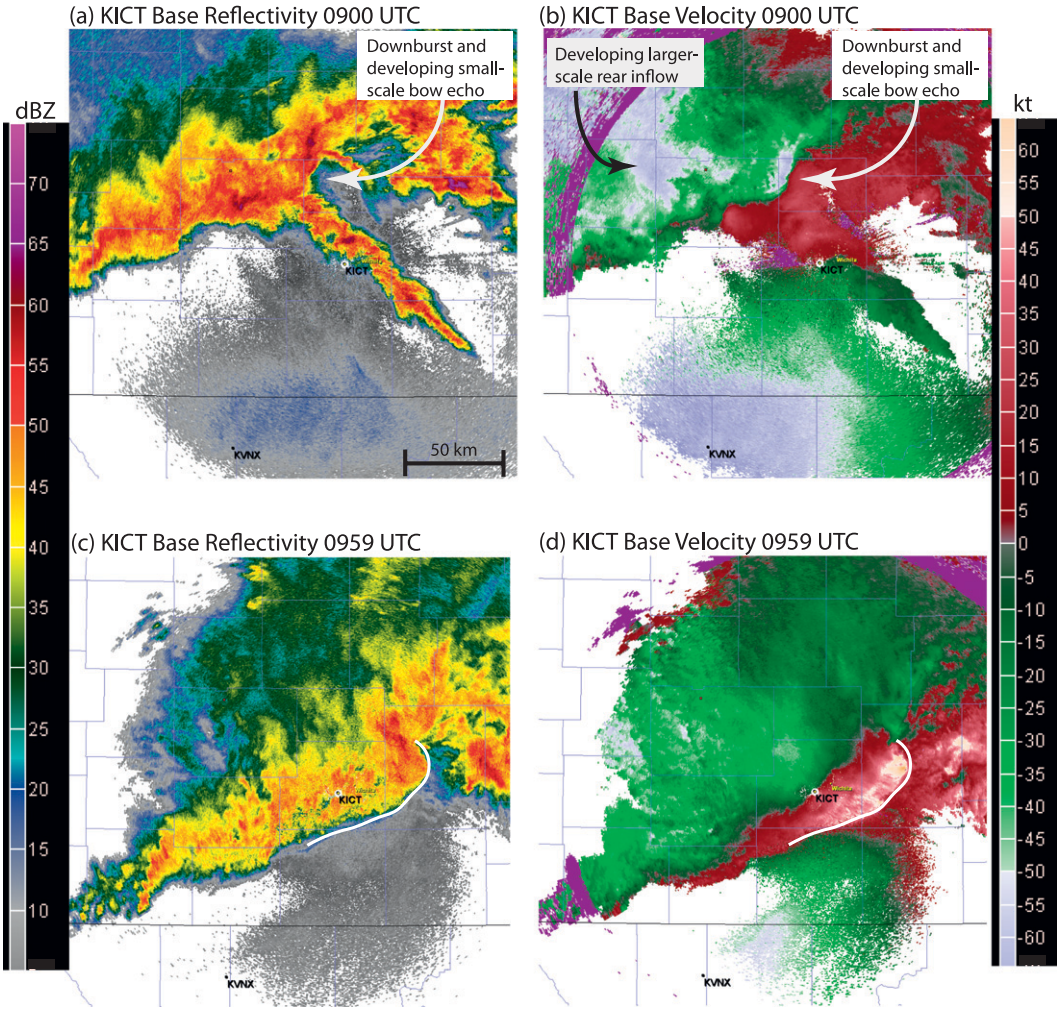

FIG. 14. Base (0.5°) reflectivity and radial velocity from KICT at 0900 and 0959 UTC. (a),(b) Features discussed in the text are indicated with annotations. (c),(d) The expanding bow echo is outlined.

4. Summary and conclusions

The wind shear in the 8 May 2009 derecho environment was very complex and departed greatly from the simpler environments that are often explored in the MCS modeling literature. While it is difficult to unravel the physical mechanisms that contributed to the development of a large, bowing MCS, the unusual mesoscale environment on 8 May 2009 documented in Coniglio et al. (2011), along with the analysis of the vertical wind shear presented in this study, suggest that many factors controlled the system strength and structure, and that the interaction of the shear over the lowest 3 km with the cold pool may not have been primary. Simulated squall lines that strongly depend on the RKW concepts, especially those that confine the shear layer to the approximate depth of the cold pool, require significant low-level line-normal shear to develop strong, persistent bow echoes. In this case, the portion of the convective line that developed into a strong bow echo had the smallest (largest) shear below (above) 3 km ahead of the line. Significant near-surface-based line-normal shear was found when looking over deeper layers (0.5–6 km), but the shear above ~3 km was responsible for much of this deeper shear ahead of the bow echo.

CCK11 proposed that the configuration of unusual mesoscale environmental features, including anomalously large inflow of very moist air and the anomalously large lapse rates in the 3–6-km layer, supported unusually large updraft mass fluxes and contributed to the strength of this event. At smaller scales, it is hypothesized that these unusual features acted in concert with the line-normal vertical wind shear in the 3–6-km layer to maintain strong convection along the spreading cold pool, to compensate for the small line-perpendicular shear in the lowest 3 km.

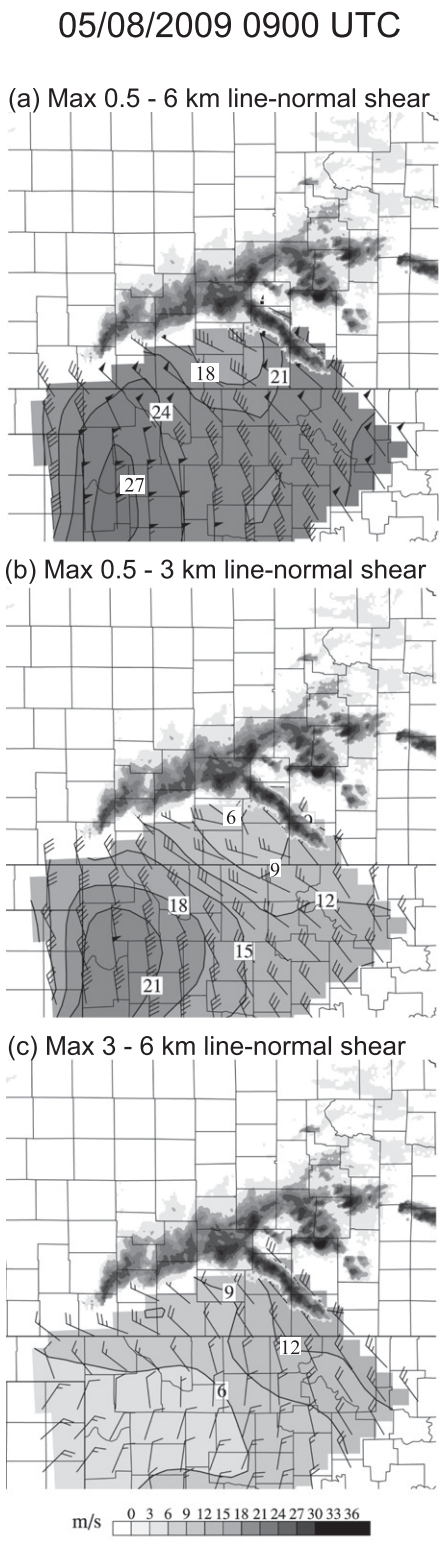

FIG. 15. As in Fig. 4, but valid at 0900 UTC 8 May 2009.

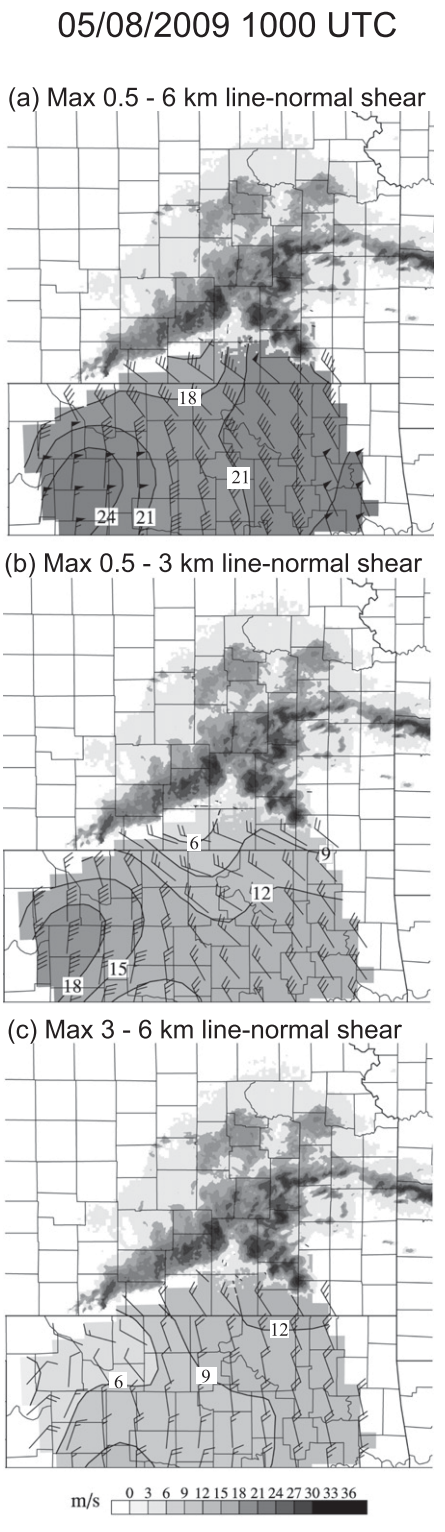

FIG. 16. As in Fig. 4, but valid at 1000 UTC 8 May 2009.

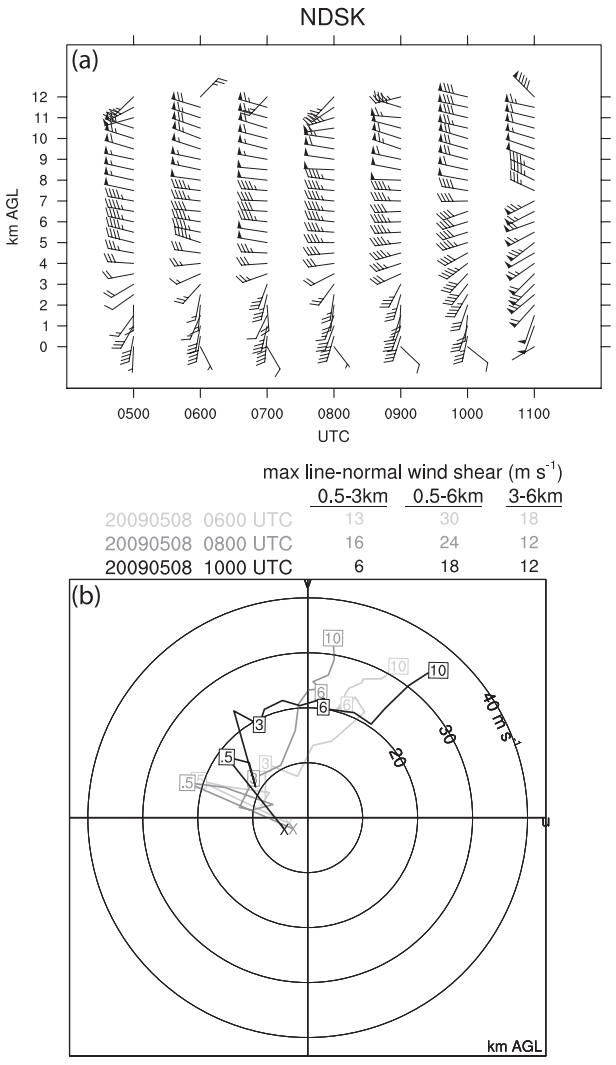

FIG. 17. As in Fig. 9, but at NDSK and valid (a) between 0500 and 1100 UTC and (b) at 0600, 0800, and 1000 UTC. Convection that developed ahead of the main MCS contaminated the wind profile at 1100 UTC.

Although the line-normal component of the low-level shear vectors below 3 km was relatively small, there was still a substantial component of the low-level shear that was line parallel. The numerical modeling studies that were used to develop and refine RKW theory explore the parameter space of instability and wind shear in idealized environments with no horizontal heterogeneity, no mesoscale or large-scale forcing, limited convective inhibition, relatively simple environmental shear profiles, and in a limited range of thermodynamic conditions (Stensrud et al. 2005). Under these conditions, simulated convective systems quickly reorient themselves perpendicular to the low-level shear, regardless of the initial orientation of the shear and the initiating mechanism for the convection (WR04; Parker and Johnson 2004).

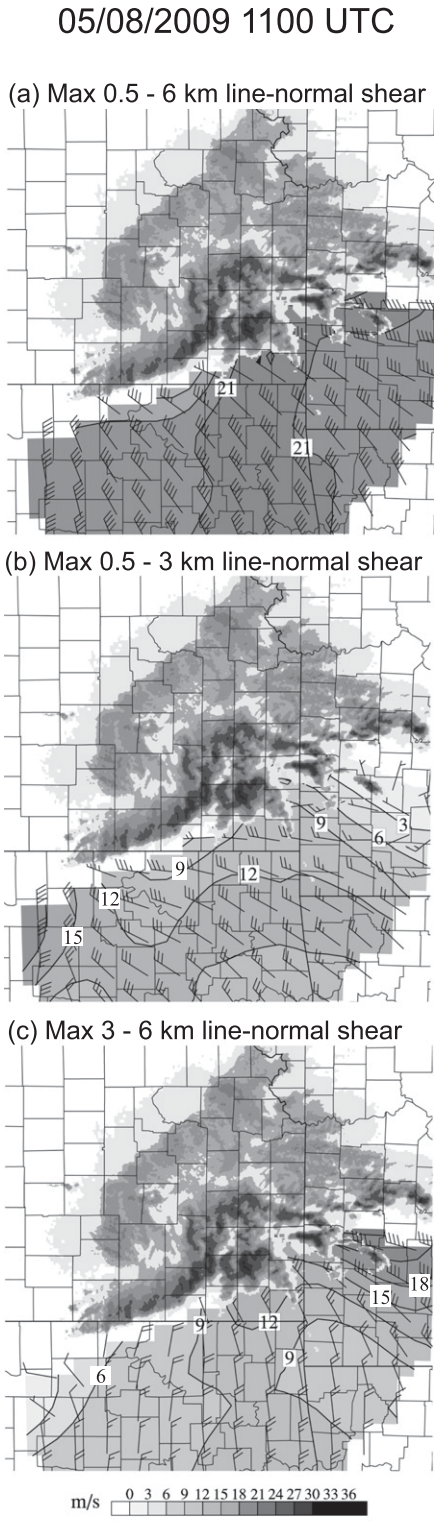

FIG. 18. As in Fig. 4, but valid at 1100 UTC 8 May 2009.

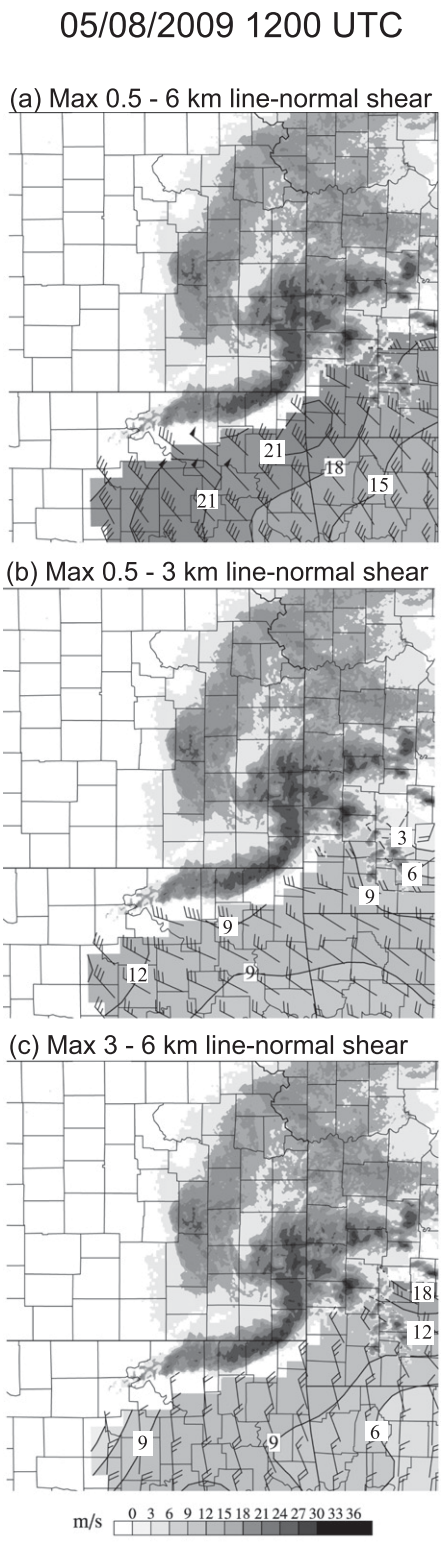

FIG. 19. As in Fig. 4, but valid at 1200 UTC 8 May 2009.

This, presumably, renders an examination of the mechanisms responsible for leading line–trailing stratiform MCSs in line-parallel low-level shear in idealized numerical simulations very difficult.

Furthermore, recent evidence suggests that the range of thermodynamic conditions typically used in the idealized MCS modeling literature may often exclude the strong and deep cold pools that can occur in the central United States (Bryan et al. 2005; Engerer et al. 2008). Modeling studies like those of Trier et al. (2006), James and Markowski (2010), and French and Parker (2010) are beginning to clarify the relevance of RKW concepts and other forcing mechanisms in these environments, but this remains an open area of research. Questions on applying the RKW concepts for deeper cold pools are raised in section 2 of the current paper. For the 8 May 2009 event, although the surface conditions did not indicate that the cold pool was especially strong, it is possible that it extended well above 3 km, in which case the strength of the system is more consistent with the predictions of RKW theory for the magnitudes of shear that are found when looking over deeper layers.

Finally, we recognize that RKW theory provides a firm basis for explaining why convection is favored on the downshear side of cold pools and for understanding the basic relationships between shear and cold pools for squall lines in simple environments. However, we believe RKW theory needs to be applied very carefully, especially as a basis for MCS prediction in complex situations with significant mesoscale forcing and kinematic and thermodynamic profiles that differ greatly from daytime heated boundary layers. A careful analysis of the environmental shear profile for the 8 May 2009 event presented herein and in CCK11 suggests that the interaction of the cold pool and the low-level shear in the lowest 3 km was not a primary factor in the strength, structure, and longevity of the system. If convective-scale effects like the cold pool–shear interactions described by RKW theory were critical in this event, then the existence of near-surface-based shear to levels above 3 km appear to have been critical. It is not clear if the RKW concepts or other processes hypothesized herein were operating under this regime of deeper shear or if the mesoscale factors highlighted in CCK11 were more important. Nonetheless, this study highlights and re-emphasizes that the deeper shear should be given more weight than 0–3-km shear in attempting to apply RKW theory and, especially, in the forecasting of MCSs in complex environments like that of 8 May 2009.

Acknowledgments. The authors thank Jason Levit, Andy Dean, and Jay Liang of the SPC who archived the SPC operational data stream for this case, which allowed

for an efficient inspection of the data for this study. We also thank Drs. David Stensrud and Matthew Parker for comments that supported expanding on the analysis of wind shear that was originally part of Coniglio et al. (2011). We also thank Dr. Parker, Dr. Stan Trier, and Dr. George Bryan for their very thorough and challenging reviews, which led to a much-improved paper. We thank Patrick Marsh, who provided help in using the GR2 analyst software, which helped us analyze the convective evolution in great detail (Fig. 14 was created using this software).

REFERENCES

Adams-Selin, R. D., and R. H. Johnson, 2010: Mesoscale surface pressure and temperature features associated with bow echoes. *Mon. Wea. Rev.,* **138,** 212–227.

Augustine, J. A., and F. Caracena, 1994: Lower-tropospheric precursors to nocturnal MCS development over the central United States. *Wea. Forecasting,* **9,** 116–135.

Benjamin, S. G., and Coauthors, 2004: An hourly assimilation–forecast cycle: The RUC. *Mon. Wea. Rev.,* **132,** 495–518.

Bryan, G. H., and M. D. Parker, 2010: Observations of a squall line and its near environment using high-frequency rawinsonde launches during VORTEX2. *Mon. Wea. Rev.,* **138,** 4076–4097.

——, D. Ahijevych, C. A. Davis, and M. L. Weisman, 2004: An assessment of convective system structure, cold pool properties, and environmental shear using observations from BAMEX. Preprints, *22nd Conf. on Severe Local Storms,* Hyannis, MA, Amer. Meteor. Soc., 4.2. [Available online at [http://ams.confex.com/ams/pdfpapers/81470.pdf.]

——, ——, ——, and ——, 2005: Observations of cold pool properties in mesoscale convective systems during BAMEX. Preprints, *11th Conf. on Mesoscale Processes/32nd Conf. on Radar Meteorology,* Albuquerque, NM, Amer. Meteor. Soc., JP5J.12. [Available online at http://ams.confex.com/ams/pdfpapers/96718.pdf.]

——, J. C. Knievel, and M. D. Parker, 2006: A multimodel assessment of RKW theory's relevance to squall-line characteristics. *Mon. Wea. Rev.,* **134,** 2772–2792.

Cohen, A. E., M. C. Coniglio, S. F. Corfidi, and S. J. Corfidi, 2007: Discrimination of mesoscale convective system environments using sounding observations. *Wea. Forecasting,* **22,** 1045–1062.

Coniglio, M. C., and D. J. Stensrud, 2001: Simulation of a progressive derecho using composite initial conditions. *Mon. Wea. Rev.,* **129,** 1593–1616.

——, ——, and M. B. Richman, 2004: An observational study of derecho-producing convective systems. *Wea. Forecasting,* **19,** 320–337.

——, ——, and L. J. Wicker, 2006: Effects of upper-level shear on the structure and maintenance of strong quasi-linear convective systems. *J. Atmos. Sci.,* **63,** 1231–1252.

——, H. E. Brooks, S. J. Weiss, and S. F. Corfidi, 2007: Forecasting the maintenance of quasi-linear mesoscale convective systems. *Wea. Forecasting,* **22,** 556–570.

——, J. W. Hwang, and D. J. Stensrud, 2010: Environmental factors in the upscale growth and longevity of MCSs derived from Rapid Update Cycle analyses. *Mon. Wea. Rev.,* **138,** 3514–3539.

——, S. F. Corfidi, and J. S. Kain, 2011: Environment and early evolution of the 8 May 2009 derecho-producing convective system. *Mon. Wea. Rev.,* **139,** 1083–1102.

Corfidi, S. F., 2003: Cold pools and MCS propagation: Forecasting the motion of downwind-developing MCSs. *Wea. Forecasting,* **18,** 997–1017.

Davis, C., and Coauthors, 2004: The Bow Echo and MCV Experiment: Observations and opportunities. *Bull. Amer. Meteor. Soc.,* **85,** 1075–1093.

Engerer, N. A., D. J. Stensrud, and M. C. Coniglio, 2008: Surface characteristics of observed cold pools. *Mon. Wea. Rev.,* **136,** 4839–4849.

Evans, J. S., and C. A. Doswell III, 2001: Examination of derecho environments using proximity soundings. *Wea. Forecasting,* **16,** 329–342.

Fankhauser, J. C., G. M. Barnes, and M. A. LeMone, 1992: Structure of a midlatitude squall line formed in strong unidirectional shear. *Mon. Wea. Rev.,* **120,** 237–260.

Fovell, R. G., and P. S. Dailey, 1995: The temporal behavior of numerically simulated multicell-type storms. Part I: Modes of behavior. *J. Atmos. Sci.,* **52,** 2073–2095.

——, and P.-H. Tan, 1998: The temporal behavior of numerically simulated multicell-type storms. Part II: The convective cell life cycle and cell regeneration. *Mon. Wea. Rev.,* **126,** 551–577.

French, A. J., and M. D. Parker, 2010: The response of simulated nocturnal convective systems to a developing low-level jet. *J. Atmos. Sci.,* **67,** 3384–3408.

Fritsch, J. M., and G. S. Forbes, 2001: Mesoscale convective systems. *Severe Convective Storms, Meteor. Monogr.,* No. 50, Amer. Meteor. Soc., 323–357.

Gale, J. J., W. A. Gallus Jr., and K. A. Jungbluth, 2002: Toward improved prediction of mesoscale convective system dissipation. *Wea. Forecasting,* **17,** 856–872.

Grady, R. L., and J. Verlinde, 1997: Triple-Doppler analysis of a discretely propagating, long-lived, high plains squall line. *J. Atmos. Sci.,* **54,** 2729–2748.

Houze, R. A., Jr., S. A. Rutledge, M. I. Biggerstaff, and B. F. Smull, 1989: Interpretation of Doppler weather radar displays of midlatitude mesoscale convective systems. *Bull. Amer. Meteor. Soc.,* **70,** 608–619.

James, R. P., and P. M. Markowski, 2010: A numerical investigation of the effects of dry air aloft on deep convection. *Mon. Wea. Rev.,* **138,** 140–161.

Johns, R. H., and W. D. Hirt, 1987: Derechos: Widespread convectively induced windstorms. *Wea. Forecasting,* **2,** 32–49.

Klemp, J. B., and R. B. Wilhelmson, 1978: The simulation of three-dimensional convective storm dynamics. *J. Atmos. Sci.,* **35,** 1070–1096.

Maddox, R. A., 1983: Large-scale conditions associated with midlatitude, mesoscale convective complexes. *Mon. Wea. Rev.,* **111,** 1475–1493.

Mahoney, K. M., G. M. Lackmann, and M. D. Parker, 2009: The role of momentum transport in the motion of a quasi-idealized mesoscale convective system. *Mon. Wea. Rev.,* **137,** 3316–3338.

Markowski, P., and Y. Richardson, 2010: *Mesoscale Meteorology in Midlatitudes*. Wiley-Blackwell, 407 pp.

Miller, D. J., and R. H. Johns, 2000: A detailed look at extreme wind damage in derecho events. Preprints, *20th Conf. on Severe Local Storms,* Orlando, FL, Amer. Meteor. Soc., 52–55.

Nolan, R. H., 1959: A radar pattern associated with tornadoes. *Bull. Amer. Meteor. Soc.,* **40,** 277–279.

Ogura, Y., and M.-T. Liou, 1980: The structure of a midlatitude squall line: A case study. *J. Atmos. Sci.,* **37,** 553–567.

Parker, M. D., 2010: Relationship between system slope and updraft intensity. *Mon. Wea. Rev.,* **138,** 3572–3578.

——, and R. H. Johnson, 2004: Structures and dynamics of quasi-2D mesoscale convective systems. *J. Atmos. Sci.,* **61,** 545–567.

Rotunno, R., and J. B. Klemp, 1982: The influence of the shear-induced pressure gradient on thunderstorm motion. *Mon. Wea. Rev.,* **110,** 136–151.

——, ——, and M. L. Weisman, 1988: A theory for strong, long-lived squall lines. *J. Atmos. Sci.,* **45,** 463–485.

——, ——, and ——, 1990: Comments on ''A numerical investigation of the organization and interaction of the convective and stratiform regions of tropical squall lines.'' *J. Atmos. Sci.,* **47,** 1031–1033.

Shapiro, A., 1992: A hydrodynamical model of shear flow over semi-infinite barriers with application to density currents. *J. Atmos. Sci.,* **49,** 2293–2305.

Smull, B. F., and R. A. Houze, 1987: Rear inflow in squall lines with trailing stratiform precipitation. *Mon. Wea. Rev.,* **115,** 2869–2889.

Stensrud, D. J., M. C. Coniglio, R. P. Davies-Jones, and J. S. Evans, 2005: Comments on '''A theory for strong long-lived squall lines' revisited.'' *J. Atmos. Sci.,* **62,** 2989–2996.

Trier, S. B., C. A. Davis, D. A. Ahijevych, M. L. Weisman, and G. H. Bryan, 2006: Mechanisms supporting long-lived episodes of propagating nocturnal convection within a 7-day WRF model simulation. *J. Atmos. Sci.,* **63,** 2437–2461.

UCAR, cited 2010a: Mesoscale convective systems: Squall lines and bow echoes. COMET Program, Boulder, CO. [Available online at https://www.meted.ucar.edu/training_module.php?id=18.]

——, cited 2010b: Severe convection II: Mesoscale convective systems. COMET Program, Boulder, CO. [Available online at https://www.meted.ucar.edu/training_module.php?id=155.]

Vasiloff, S. V., and Coauthors, 2007: Improving QPE and very short term QPF: An initiative for a community-wide integrated approach. *Bull. Amer. Meteor. Soc.,* **88,** 1899–1911.

Weisman, M. L., 1992: The role of convectively generated rear-inflow jets on the evolution of long-lived mesoconvective systems. *J. Atmos. Sci.,* **49,** 1826–1847.

——, 1993: The genesis of severe, long-lived bow echoes. *J. Atmos. Sci.,* **50,** 645–670.

——, 2001: Bow echoes: A tribute to T. T. Fujita. *Bull. Amer. Meteor. Soc.,* **82,** 97–116.

——, and R. Rotunno, 2004: ''A theory for strong, long-lived squall lines'' revisted. *J. Atmos. Sci.,* **61,** 361–382.

——, and ——, 2005: Reply. *J. Atmos. Sci.,* **62,** 2997–3002.

——, J. B. Klemp, and R. Rotunno, 1988: Structure and evolution of numerically simulated squall lines. *J. Atmos. Sci.,* **45,** 1990–2013.

Wheatley, D. M., R. J. Trapp, and N. T. Atkins, 2006: Radar and damage analysis of severe bow echoes during BAMEX. *Mon. Wea. Rev.,* **134,** 791–806.